Upgrading of furfural to biofuel precursors via aldol condensation with acetone over magnesium hydroxide fluorides MgF 2–x (OH)x

Minrui Xu, Stephane Celerier, Jean-Dominique Comparot, Julie Rousseau, Matthieu Corbet, Frederic Richard, Jean-Marc Clacens

ARTICLE

Upgrading of furfural to biofuel precursors via aldol condensation with acetone over magnesium hydroxide fluorides $MgF_{2-x}(OH)_x$

Received 00th January 20xx,
Accepted 00th January 20xx

DOI: 10.1039/x0xx00000x

Minrui Xu [a], Stéphane Célerier *[a], Jean-Dominique Comparot [a], Julie Rousseau [a], Matthieu Corbet [b], Frédéric Richard *[a], Jean-Marc Clacens [a]

Wastes from ligno-cellulosic material, especially hemicellulose, are extremely promising resources to produce fuels from renewable raw materials. Furfural, resulting from the depolymerization of hemicellulose, is often considered as an extremely interesting platform molecule. Particularly, new biofuels containing molecules with 8 and 13 carbon atoms can be produced from aldol condensation of furfural and acetone followed by a deoxygenation reaction. In this work, several magnesium hydroxide fluorides $MgF_{2-x}(OH)_x$ were prepared by a sol-gel method with various F/Mg ratios (0 to 2) at 100 °C. All solid samples were fully characterized by several technics (nitrogen adsortion-desorption, TEM, IR, XRD and ICP). $MgF_{2-x}(OH)_x$ were mainly composed of an intimate mixture of MgF_2 and $Mg(OH)_{2-x}(OCH_3)_x$ and exhibited both acid-base properties and high surface area. From CO_2 adsorption experiments, a basicity scale corresponding to basic sites with moderate strength was established: $MgF_{1.5}(OH)_{0.5}$ > MgF(OH) ~ $MgF_{1.75}(OH)_{0.25}$ > $MgF_{0.5}(OH)_{1.5}$ > $Mg(OH)_2$ >> MgF_2. It was proposed that the presence of fluorine allowed to stabilize the basic sites with moderate strength at ambient atmosphere. The aldol condensation of furfural and acetone was carried out under mild reaction conditions (50 °C, P_{atm}) over $MgF_{2-x}(OH)_x$. These catalysts were involved in this reaction without using classical activation step for basic solid catalysts, which constitutes a major advantage for energy saving and thus, economical efficiency. The solid with the F/Mg ratio equal to 1.5 ($MgF_{1.5}(OH)_{0.5}$) exhibited the highest activity, the furanic dimer (1,5-di(furan-2-yl)penta-1,4-dien-3-one) being the main product. A good correlation between the catalytic activity and the basicity scale was highlighted. Based on these results, the nature of active sites was proposed: a combination of a Lewis acid site (coordinatively unsaturated metal site) in the vicinity of a basic site (hydroxyl groups of $Mg(OH)_{2-x}(OCH_3)_x$). The effect of the furfural/acetone ratio on the catalytic properties of $MgF_{1.5}(OH)_{0.5}$ was also investigated.

Introduction

Nowadays environment-friendly development arouses more and more attention to the public. For instance, extensive efforts are made to replace petroleum resources by renewable biomass-derived chemicals.[1,2] Among the main components of agricultural wastes, lignocellulose remains the most abundant biomass.[3] Hemicellulose, representing about 25% of lignocellulose, can be considered as a precursor of furfural, a promising biomass-derived platform molecule, mainly obtained by acid-catalyzed dehydration of xylose.[4–6]

Since the research of bio-based building block synthesis from furfural continues to burgeon, multifarious value-added compounds were produced from furfural.[7–11] The synthesis of new types of biofuels can also be considered from furfural, involving aldol condensation and hydrodeoxygenation reactions.[12–16] Aldol condensation reactions play a crucial role in the upgrading of furfural since this approach increases the carbon chain length by forming new C-C bonds. Especially, the aldol condensation of furfural and acetone leads to products containing either 8 (4-(furan-2-yl)but-3-en-2-one, FAc) or 13 carbon atoms (1,5-di(furan-2-yl)penta-1,4-dien-3-one, F_2Ac), as described in scheme 1.[11] In addition, their hydrodeoxygenation were studied over metallic based catalysts to upgrade these compounds as renewable fuels.[17–20]

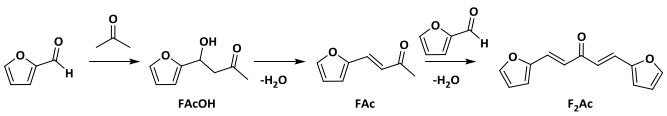

Scheme 1: Schematic illustration of adol condensation between furfural and acetone

Generally, sodium hydroxide is a well-known homogeneous basic catalyst for aldol condensation. For example, Fakhfakh et al.[21] obtained a mixture containing FAc and F_2Ac in equimolar amounts when a total conversion of furfural was reached under mild experimental conditions (40 °C, atmospheric pressure).

[a] Institut de Chimie des Milieux et Matériaux de Poitiers, UMR 7285 Université de Poitiers - CNRS, 4 rue Michel Brunet, BP633, 86022 Poitiers Cedex, France. E-mail : stephane.celerier@univ-poitiers.fr, frederic.richard@univ-poitiers.fr
[b] Solvay Research & Innovation center of Lyon, 85 rue des Frères Perret, BP 62 69192, Saint Fons, France

Electronic Supplementary Information (ESI) available: [details of any supplementary information available should be included here]. See DOI: 10.1039/x0xx00000x

Nevertheless, the use of such catalyst leads to many drawbacks, especially due to its high corrosiveness. In addition, homogeneous catalytic processes commonly encounter disadvantages, including the neutralization of reaction mixture producing wastes and the difficulty of catalysts separation. This reaction was also studied over solid catalysts possessing basic properties such as metal oxides.[22–25] For example, Shen et al.[22] obtained a high conversion of furfural (90%) with a selectivity on furanic dimer (F_2Ac) close to 65% over MgO-ZrO_2 in presence of a furfural/acetone molar ratio equal to 1 under drastic experimental conditions (120 °C and 5.2 MPa). Under milder conditions (60 °C, atmospheric pressure) and in presence of an excess of acetone (furfural/acetone molar ratio close to 0.1), a high conversion of furfural (about 70%) was also reached over MgO-ZrO_2 mixed oxide catalysts.[23] The alcohol intermediate (4-(furan-2-yl)-4-hydroxybutan-2-one, FAcOH) was always the main product, whereas the selectivity of F_2Ac was always less than 10 mol%, irrespective to the furfural conversion. Over the same type of catalyst at 50 °C but under nitrogen pressure (1 MPa), a conversion of furfural close to 80% was obtained by using an equimolar mixture of acetone and furfural.[24] In this case, the reaction mixture was mainly composed by F_2Ac (75 mol% in selectivity). In presence of a mesoporous TiO_2 catalyst exhibiting both basic and acid sites, a low conversion of furfural was obtained (25%) at 50 °C.[25] Probably due to the high amount of acetone compared to furfural (furfural/acetone ratio equal to 0.2), the monomer (FAc) was the main detected product, its selectivity being higher than 70 mol%. In this case, the alcohol intermediate (FAcOH) was observed in traces due to the presence of acid sites favouring its dehydration in FAc. Due to this, solids having acidic properties were also evaluated as catalysts for this reaction, such as zeolites,[26,27] acids metal chlorides[28] and metal-organic frameworks.[29,30] For instance, a HBEA zeolite was used as catalyst for aldol condensation of furfural and acetone even if the furfural conversion was only 38% at 100 °C (furfural/acetone molar ratio equal to 0.1) as shown by Kikhtyanin et al.[26] Under these experimental conditions, as discussed above, an excess of acetone and the presence of acid sites explained that FAc was the main product detected in the reaction mixture. Nevertheless, an undesired reaction between two molecules of F_2Ac leading to a heavy product, noted $(FAc)_2$, was observed due to the presence of Brønsted acid sites. When Sn was added in the HBEA zeolite in order to promote its Lewis acidity, a very high furfural conversion (more than 90%) was reached at 160 °C (furfural/acetone molar ratio equal to 0.1).[27] FAc was the main product and the presence of $(FAc)_2$ was not mentioned. Interestingly, when acidic catalysts were used, the monomer (FAc) was always much more favored than the dimer (F_2Ac).[26–30] As a consequence, in order to favor the C13 furanic dimer (F_2Ac) instead of FAc, during the aldol condensation of furfural and acetone, the use of basic catalysts seems to be more appropriate.

In the past decade, inorganic oxide hydroxide fluorides with high specific surface area prepared by soft chemistry were developed as a new and performant class of catalyst and/or (active) support.[31,32] Such solids are known to exhibit different types of acid-base properties. As an example, aluminium hydroxide fluorides $AlF_{3-x}(OH)_x$ exhibit tuneable acid properties, with neighbouring Lewis and Brønsted acid sites. These fluorides were successfully used as catalyst for acylation of 2-methylfuran by acetic anhydride (50 °C, atmospheric pressure)[33] and for condensation of 2,3,6-trimethylhydroquinione with isophytol (100 °C, atmospheric pressure).[34] On the contrary, magnesium oxide (hydroxide) fluorides $MgF_{2-x}(OH)_x$ possess basic properties. Such solids were successfully used as either basic catalysts for the Michael addition of 2-methylcyclohexane-1,3-dione to methyl vinyl ketone (25 °C, atmospheric pressure)[35] or catalytic support.[36–40] Moreover, the use of solid basic catalysts involves generally an activation step at high temperature to active basic sites by removal of carbonate species. Find an active catalyst which does not require this activation step could be interesting for energy saving and economic point of view when the reaction is performed at low temperature.

In this work, various hydroxide fluorides $MgF_{2-x}(OH)_x$ solid samples with different F/Mg ratio were prepared by a sol-gel method according to the procedure developed by Scholz et al. [41]. The easy control of the F/Mg ratio of these materials allows to fine tune their acid-base properties. These solid materials were evaluated as catalyst without preliminary thermal activation for aldol condensation of furfural and acetone under mild conditions (50 °C, atmospheric pressure) in a batch reactor. Based on these results, the nature of active sites was discussed and a reaction mechanism was proposed.

Experimental

Synthesis of catalysts

The magnesium hydroxide fluorides $MgF_{2-x}(OH)_x$ with x = 2, 1.5, 1, 0.5, 0.25 and 0 were prepared by a sol-gel method, partly based on the work of Scholz et al.[41] In the first step, magnesium metal (3.23 g, Aldrich, 99.98%) was treated with methanol in excess (100 mL, Sigma-Aldrich, 99.8%) under reflux conditions for 6 h to form a $Mg(OCH_3)_2$ metal alkoxide solution. Various volumes of aqueous HF (48 wt% HF in water, Sigma-Aldrich, 99.99%) were added progressively under stirring conditions to obtain several HF/Mg molar ratios, ranging from 0.5 to 2. The amount of water (provided from aqueous HF or/and additional water) was adjusted to obtain in each case a H_2O/Mg ratio of 2 to favor the hydrolysis of remaining OCH_3 groups. A highly exothermic reaction occurred to obtain a sol. This sol was stirred for 24 h, aged at ambient temperature for 24 h and dried at 100 °C for 24 h. According to this synthesis procedure, five solids named MgF_2, $MgF_{1.75}(OH)_{0.25}$, $MgF_{1.5}(OH)_{0.5}$, MgF(OH) and $MgF_{0.5}(OH)_{1.5}$ were obtained with the initial HF/Mg molar ratio of 2, 1.75, 1.5, 1 and 0.5, respectively. To synthesize the sample named $Mg(OH)_2$, the protocol was the same except that the aqueous HF solution was replaced by water (initial H_2O/Mg molar ratio equal to 2.5).

Catalyst characterizations

The magnesium composition of each catalyst was determined by inductively coupled plasma optical emission spectrometry (ICP-OES) using a PerkinElmer Optima 2000DV instrument. The fluorine content was measured by ionic chromatography (DIONEX ICS-2000).

X-ray diffraction (XRD) patterns were collected between 2θ = 5 and 75° using a PANalytical EMPYREAN powder diffractometer using Cu-Kα monochromatized radiation source (Kα = 1.54059 Å) with a 0.1° step and 600s dwell time. Phase identification was performed by comparison with the ICDS database reference files.

The textural properties were determined from N_2 adsorption-desorption isotherms, which were measured using a TRISTAR 3000 gas adsorption system at -196 °C. Prior to N_2 adsorption, the samples were degassed overnight under secondary vacuum at 90 °C. The specific surface area (S_{BET} in $m^2\ g^{-1}$) was calculated from the adsorption isotherm (P/P_0 between 0.05 and 0.20) using the Brunauer-Emmett-Teller (BET) method. The total pore volume was calculated from the adsorbed volume of nitrogen at P/P_0 equal to 0.99. The average mesopore-size distribution was calculated from the desorption isotherm branch using the Barret-Joyner-Halenda (BJH) method.

The measurement of the basicity was obtained by adsorption of CO_2 followed by FTIR spectroscopy using a ThermoNicolet NEXUS 5700 spectrometer (resolution of 2 cm^{-1} and 128 scans per spectrum). Solid samples were pressed into thin pellets (15-30 mg) with diameter of 16 mm under a pressure of 1-2 t cm^{-2} and activated in situ during two hours under secondary vacuum (2 10^{-6} bar) at 90 °C. After cooling down the samples until room temperature, CO_2 was introduced in the cell, which was placed under vacuum and heated at 50 °C to remove physisorbed CO_2. Finally, IR spectrum was recorded and normalized at the same mass for each sample. The measurement of the acidity of all solid samples was obtained by adsorption of CO followed by FTIR spectroscopy. Experiments were carried out with the same equipment and the same activation procedure (90°C) such as those used for CO_2 adsorption experiments. The cell was cooled down with liquid nitrogen to -173 °C. Then successive doses of CO were introduced quantitatively and a spectrum was recorded after each adsorption until saturation. The final spectrum was recorded with 1 Torr of CO at equilibrium pressure (saturation). All spectra were normalized at the same mass of magnesium hydroxide fluoride samples (20 mg).

Transmission Electronic Microscopy (TEM) experiments were carried out using a JEOL 2100 instrument (operated at 200 kV with a LaB6 source and equipped with a Gatan Ultra scan camera) coupled with an Energy Dispersive X-ray Spectrometer (EDS) allowing the determination of F, O, C and Mg contents. For EDS measurements, 10-15 analyses were performed for each studied samples (MgF_2, $Mg(OH)_2$ and MgF(OH)) to obtain an average value. SAED (Selected area electron diffraction) experiments were also performed.

Catalytic procedure for aldol condensation of furfural and acetone

The reaction was carried out in a batch reactor fitted with a magnet stirrer and heated at 50 °C. The catalyst (200 mg) was introduced in a mixture composed of furfural (5 mmol, Sigma–Aldrich, 99%, preliminarily distilled), acetone (10 mmol, 5 mmol or 2.5 mmol, Sigma–Aldrich, >99%), heptane (7.5 mmol, Sigma–Aldrich, 99%) and 2-methyltetrahydrofuran as solvent (5 mL, Alfa Aesar, 99%). Heptane, inert in these conditions, was used as an internal standard for quantitative analysis carried out by Gas Chromatography. Each liquid sample obtained after various reaction times (between 30 and 360 min) was analysed by using a Varian 430 chromatograph equipped with CPSIL–5CB capillary column (length: 50 m; diameter: 0.25 mm, film thickness: 0.4 μm) and a flame ionization detector. The oven temperature was programmed from 70 °C to 150 °C (5 °C min^{-1}), then from 150 °C to 250 °C (10 °C min^{-1}) and maintained at 250 °C during 10 minutes. All detected products were identified by co-injection of commercial samples and/or by using Varian 3800 chromatograph coupled with a 1200 TQ mass spectrometer.

The conversion of furfural (X_F in %) and the yield in each product (Y in mol%) were calculated using the following equations, according to O'Neill et al. :[42]

$$X_F = \frac{C_{F,0} - C_F}{C_{F,0}} . 100 \quad (1)$$

$$Y_{FAcOH} = \frac{C_{FAcOH}}{C_{F,0}} . 100 \quad (2)$$

$$Y_{FAc} = \frac{C_{FAc}}{C_{F,0}} . 100 \quad (3)$$

$$Y_{F_2Ac} = \frac{2.C_{F2Ac}}{C_{F,0}} . 100 \quad (4)$$

with $C_{F,0}$ being the initial concentration of furfural, C_F, C_{FAcOH}, C_{FAC} and C_{F2Ac} being the concentrations of various compounds determined at a given reaction time. Whatever the catalysts, the molar balance carbon is between 95 and 100%.

Results and discussion

Characterization of the catalysts

The so-called $Mg(OH)_2$ sample was prepared by a sol gel method without added HF aqueous solution during the synthesis. The XRD pattern of this solid exhibited broad peaks highlighting a low rate of crystallinity (Fig. 1).

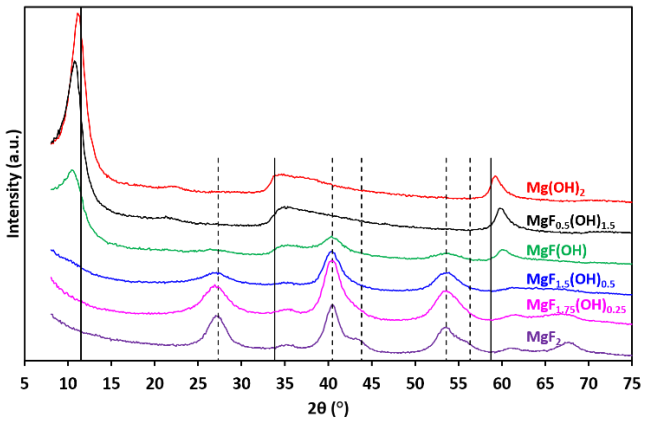

Fig. 1 X-ray diffraction patterns of $MgF_{2-x}(OH)_x$ samples. Dotted lines: mean diffraction peaks of MgF_2 (JCPDS file N° 01-070-2268); solid lines: main diffraction peaks of $Mg(OH)_{1.3}(OCH_3)_{0.7}$ (JCPDS file N°00-022-1788)

As expected, the formation of layered-methoxide of magnesium with the $Mg(OH)_{2-x}(OCH_3)_x$ formula was observed attesting that the hydrolysis of magnesium alkoxide by water was incomplete even if water was added in excess, in agreement with Rywak et al. [43] A weak shift towards lower angles of the peaks was observed in comparison with the peaks of the JCPDS file of the $Mg(OH)_{1.3}(OCH_3)_{0.7}$ material. This composition is probably not entirely the same as our synthetized material explaining this shift. This solid sample exhibited a microstructure composed of crumpled sheets as shown by transmission electron microscopy (Fig. 2). The observation of sheets is in accordance with the formation of layered-methoxide magnesium as observed by XRD (Fig. 1). As expected from the stoichiometry of this sample ($Mg(OH)_{2-x}(OCH_3)_x$), the O/Mg ratio determined by EDS was close to 2.0. Using the same technic, the carbon content of this material was also evaluated. Indeed, a value of x corresponding to the number of OCH_3 groups was approximately ranged between 0.5 and 0.9, close to the reference indicated in XRD patterns (equal to 0.7). The presence of such methoxy groups was confirmed by FT-IR (Fig. 3). Indeed, the bands between 2800 and 2950 cm^{-1} can be assigned to OCH_3 groups.[44]

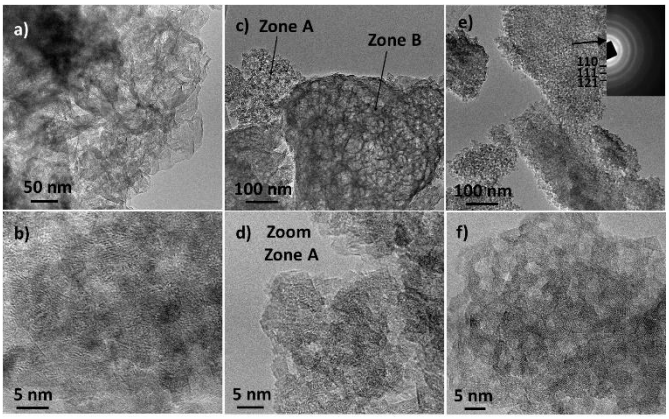

Fig. 2 TEM images of $Mg(OH)_2$ (a and b), MgF(OH) (c and d) and MgF_2 (e and f). Corresponding SAED pattern (insert image) of picture e

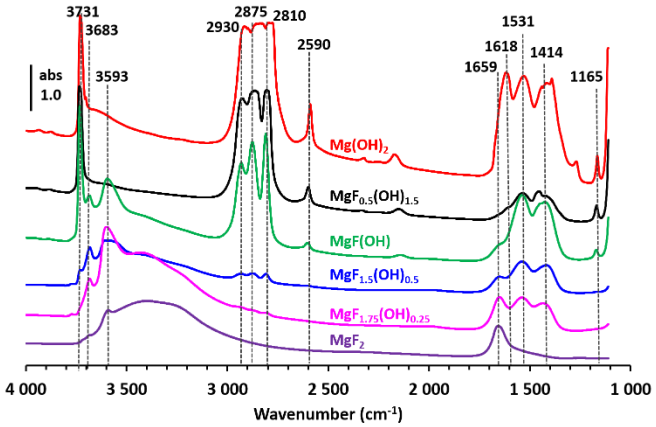

Fig. 3: IR spectra of $MgF_{2-x}(OH)_x$ samples after activation at 90 °C under vacuum

When an initial HF/Mg ratio equal to 2 was used during the synthesis, the solid corresponds to MgF_2 crystallographic phase as shown by XRD (Fig 1). The F/Mg molar ratio was determined by a combination of ICP-OES for Mg content, and ionic chromatography for F content. The value, given in Table 1, is in agreement with the expected one. This solid sample can be defined by a homogeneous porous structure composed of small crystallites of 4-7 nm as observed by TEM (Fig. 2). The F/Mg ratio determined by EDS was close to 2.1 whatever the analysed region attesting the formation of MgF_2. From the corresponding energy-filtered SAED pattern, d spacing of 3.4, 2.2 and 1.7 Å were determined and corresponded to (110), (111) and (121) diffraction planes of MgF_2.

Several magnesium hydroxide fluorides solids $MgF_{2-x}(OH)_x$, with x equal to 0.25, 0.5, 1, 1.5 and 1.75, were also prepared by a sol-gel method as described in the experimental part. For each solid sample, the experimental F/Mg ratio was close to the target value (Table 1). In these conditions, a competition between fluorolysis (reaction with HF) and hydrolysis (reaction with H_2O) occurred. As the rate of the former reaction being higher, the fluorine content in the magnesium hydroxide fluoride is easily tuned and reasonably controlled by the initial HF/Mg molar ratio thanks to this sol-gel method and increases linearly with the amount of HF added, in agreement with results reported by Prescott et al. [35] In these samples, at least two crystallographic phases can be detected (Fig. 1). For example, the XRD pattern of MgF(OH) sample exhibited the peaks of both MgF_2 and $Mg(OH)_{2-x}(OCH_3)_x$ phases. As expected, higher the initial HF/Mg molar ratio used in solid synthesis is, higher the contribution of the MgF_2 phase in the considered pattern is at the expense of $Mg(OH)_{2-x}(OCH_3)_x$ phase.

Table 1: Physico-chemical properties of magnesium hydroxide fluoride $MgF_{2-x}(OH)_x$ samples

Catalyst	F/Mg ratio[1]	S_{BET}[2] ($m^2\ g^{-1}$)	V_{pore}[3] ($cm^3\ g^{-1}$)	d_{pore}[4] (nm)	Basicity[5] (a.u.)
$Mg(OH)_2$	0	313	0.56	6.1	0.005
$MgF_{0.5}(OH)_{1.5}$	0.4	630	0.73	4.5	0.039
MgF(OH)	1.1	599	0.75	5.2	0.069
$MgF_{1.5}(OH)_{0.5}$	1.6	406	0.75	7.2	0.174
$MgF_{1.75}(OH)_{0.25}$	1.8	387	0.55	6.0	0.068
MgF_2	2.0	280	0.26	4.4	0

[1] Fluor content measured by ionic chromatography and Mg content measured by ICP-OES; [2] Specific surface area measured by the BET method; [3] Total pore volume calculated at P/P_0 equal to 0.99; [4] Average pore size deduced from the BJH method using the desorption branch; [5] Determined from the area of the band at 1225 cm^{-1} obtained after activation at 90 °C under vacuum and adsorption-desorption of CO_2 at 50 °C (values deduced from spectra presented in Fig. 4)

The formation of this intimate mixture of phases was confirmed by TEM analysis (Fig. 2). As an example, two well separated zones were visible in the TEM image for the MgF(OH) sample (Fig. 2c). The zone "A" presents a microstructure comparable to MgF_2 phase given in Fig. 2f. The determined F/Mg ratio of 1.9 by EDS was close to the expected value (equal to 2). The corresponding SAED (not shown in Fig 2d) was equivalent to the one inserted in Fig. 2e. The zone "B" with crumpled sheets is similar to the $Mg(OH)_{2-x}(OCH_3)_x$ phase shown in Fig. 2b. In addition, a O/F/Mg ratio of 1.2/0.9/1 measured by EDS, indicates the presence of an intimate mixture of MgF_2 and $Mg(OH)_{2-x}(OCH_3)_x$ in the zone "B". Nevertheless, the insertion of a fraction of fluorine in $Mg(OH)_{2-x}(OCH_3)_x$ and of hydroxyl group in MgF_2 cannot be obviously excluded to form $MgF_{2-x-y}(OH)_x(OCH_3)_y$ mixed phase as already proposed.[35] Moreover, taking into account the low crystallinity of these samples showed by XRD (Fig. 1), each phase is composed of randomly-dispersed small domain leading to a very close proximity and a high amount of interfaces between them.

The adsorption-desorption isotherms of all solids are shown in Fig. S1. A type IV isotherm according to the IUPAC classification was observed for all samples whatever the fluorine content showing the formation of mesoporous solids with a pore volume between 0.3 and 0.7 $cm^3\ g^{-1}$ (Table 1). The average pore size determined by the BJH method is between 4 and 7 nm for all materials. The specific surface areas of these solids are very high (from 280 $m^2\ g^{-1}$ for MgF_2 to 630 $m^2\ g^{-1}$ for $MgF_{0.5}(OH)_{1.5}$), in accordance with the low crystallinity observed by XRD (Fig. 1). These surface areas are relatively close to the values obtained for the magnesium hydroxide fluorides prepared in similar conditions by Scholz et al.[41] Interestingly, the specific surface areas of the $MgF_{2-x}(OH)_x$ samples were drastically higher than those of MgF_2 and $Mg(OH)_2$ pure materials. The synthesis of an intimate mixture of MgF_2 and $Mg(OH)_{2-x}(OCH_3)_x$ allowed hence to obtain very high specific surface areas. This can be explained by a delay in the crystallization processes due to the presence of a second phase which affects the rate of crystallization of the first one.[36] This phenomenon is in favour of the nanoparticles formation, as observed by TEM (Fig. 2).

After their activation under secondary vacuum at 90 °C, all catalysts, initially synthesized at 100°C, were characterized by FT-IR before (Fig. 3) and after CO_2 adsorption (Fig. 4). Concerning the spectra shown in Fig. 3, the sharp band observed around 3730 cm^{-1} is assigned to $\upsilon_{(MgO-H)}$.[41] As expected, the intensity of this band decreases with the increase of the fluorine content, due to the lower amount of OH groups. According to Prescott et al.,[35] a weak band centred at 3683 cm^{-1} can be attributed to the bridging of OH groups in $MgF_{2-x}(OH)_x$ samples, especially observed when $x \leq 1$, i.e. for MgF(OH), $MgF_{1.5}(OH)_{0.5}$ and $MgF_{1.75}(OH)_{0.25}$ samples. The bands at 2930, 2870 and 2810 cm^{-1} can be attributed to $\upsilon_{(CH)}$ of the methoxy groups present in these magnesium hydroxide fluoride samples.[41] The decrease of their intensity with the increase of F content can be explained by the lower amount of $Mg(OH)_{2-x}(OCH_3)_x$ phase in the solid samples, in accordance with XRD analysis. The strong bands between 1650 and 1400 cm^{-1} originate from carbonate and hydrogen carbonate species formed by the reaction of atmospheric CO_2 with the $MgF_{2-x}(OH)_x$ materials basic sites.[35,41] The strong intensity of these bands observed for the $Mg(OH)_2$ solid can be explained by the highest basicity of such solid. In addition, adsorbed water can lead to a broad band located between 3400-3600 cm^{-1} and a sharp band around 1659 cm^{-1}, as reported by Rywak et al. [43] These bands were particularly intense on IR spectra of solids having $x \leq 0.5$, indicating that the presence of fluorine seems to favour the retention of adsorbed water. This is probably linked to the increase of the Lewis acidity of solid samples with the fluorine content as confirmed below with the characterization of acidity. It can be noted that the activation step used for IR analysis (degassing at 90°C under vacuum) was insufficient to remove all the water adsorbed on these samples.

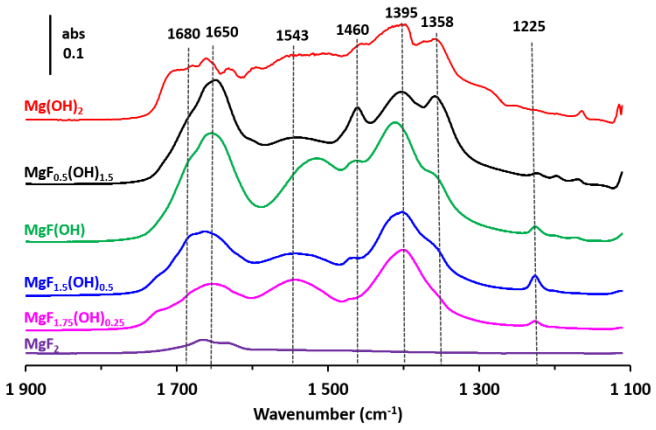

Fig. 4 Difference of IR spectra obtained after CO_2 adsorption at 50 °C and after activation at 90 °C under vacuum of $MgF_{2-x}(OH)_x$ samples with $0 \leq x \leq 2$

According to the results reported by Wuttke et al.,[45] the OH groups present on such $MgF_{2-x}(OH)_x$ materials exhibit either acidic or basic properties. This is obviously due to the stronger inductive effect of fluorine atoms in comparison to oxygen atoms. Thus, the easy control of the F/Mg ratio of these materials by sol-gel process allows to fine tune their acid-base properties. When x is low (about less than 0.1) corresponding to the so-called MgF_2 in the present

study, it was proposed that OH groups in minor quantities are Brønsted acid sites and this solid is an acidic material, exhibiting mainly Lewis acidity attributed to the presence of under coordinated Mg^{2+} species.[46,47] It can explain the absence of IR bands in the carbonate and hydrogen carbonate region (between 1350 and 1640 cm^{-1}) as shown in Fig. 3. On the contrary, with x higher than 0.1, the OH groups can be considered as basic sites. Consequently, several bands between 1350 and 1640 cm^{-1} can be observed due to reaction between hydroxyl groups and atmospheric CO_2. Besides, their intensity increased with the decrease of the fluorine content.

To deeper understand the acid-base properties of the as-synthesized $MgF_{2-x}(OH)_x$ samples, additional experiments using CO_2 adsorption-desorption procedure were carried out at 50 °C under vacuum. The spectra presented in Fig. 4 were obtained through subtraction between the spectrum realized after CO_2 adsorption followed by heating at 50 °C under vacuum and those measured after the activation procedure at 90 °C (presented in Fig. 3). As expected, no bands were observed for MgF_2 highlighting the absence of basic sites on this solid. For all other samples, several bands appeared between 1100 – 1900 cm^{-1}, showing that some basic sites remained available to adsorb CO_2 and to form carbonate and bicarbonate species.[48–50] The decrease of the fluorine content is linked to an increase of several bands, including notably those located at 1358 and 1460 cm^{-1}, which could be attributed to the presence of carbonate species. These species can be formed on strong basic sites. On the contrary, the band at 1225 cm^{-1} which corresponds to the $\delta_{(OH)}$ vibration of hydrogen carbonate species, allows to evaluate the presence of basic sites with moderate strength. The area of this band was reported in Table 1 for all solids. Surprisingly, the amount of these sites increases with the fluorine content in $MgF_{2-x}(OH)_x$ series (x in the range of 2 – 0.5), whereas the inductive effect of fluorine is rather known to decrease the basicity of the solids.[45] The higher amount of basic hydroxyl group with low strength can be explained by the higher amount of fluorine in the vicinity of this hydroxyl group leading to decrease the strength of basicity. In the case of low-fluorine-containing magnesium hydroxide fluorides, the majority of hydroxyl groups are probably basic with high strength which react with CO_2 of ambient air. Thus, the fluorine atoms included in these materials act as stabilizer of basic hydroxyl groups with low strength explaining why $MgF_{1.5}(OH)_{0.5}$ retains higher amount of basic hydroxyl groups.

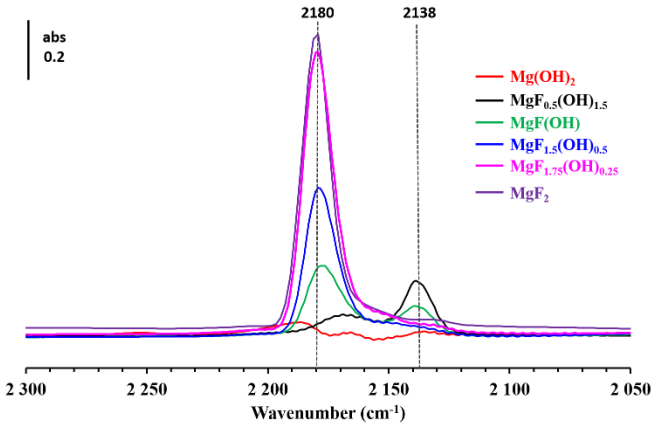

Fig. 5 Difference of IR spectra obtained after CO adsorption at saturation at -173 °C and after activation at 90 °C under vacuum of $MgF_{2-x}(OH)_x$ samples with $0 \leq x \leq 2$.

The acid properties were also determined by adsorption of CO followed by IR. CO is a suitable probe molecule for the characterization of Lewis acidity because the ν(CO) frequency is very sensitive to the local cationic environment.[51] After CO adsorption, this band shifts more or less depending on the strength of Lewis acidity: the stronger the Lewis acidity, the higher the shift. The spectra obtained after CO saturation for each catalyst are reported in Fig. 5. Except for $Mg(OH)_2$ and $MgF_{0.5}(OH)_{1.5}$, the main ν(CO) band is observed at 2180 cm^{-1} and corresponds to CO adsorbed on Lewis acid sites with moderate strength.[52,53] Taking into account that no significant shift was observed in the OH region (around 3700 cm^{-1}), which is characteristic of CO adsorption on Brønsted acid sites (not showed here),[54] we can reasonably assigned the band at 2180 cm^{-1} to an interaction of CO with Lewis acid sites. The low amount of Brønsted acidity on MgF_2 prepared in the same conditions was already observed.[47] Conversely, $Mg(OH)_2$ and $MgF_{0.5}(OH)_{1.5}$ have not or few Lewis acid sites. Only a band at 2138 cm^{-1} is observed corresponding to the weak and unspecific CO adsorption (physisorbed CO species).[53] As expected, the amount of Lewis acidity increases with the fluorine content as showed by the increase of the surface of the IR band located at 2180 cm^{-1}.

Catalytic properties of magnesium hydroxide fluorides

The activity of magnesium hydroxide fluorides were evaluated in aldol condensation of furfural (Furf) and acetone (Ac) at 50 °C under atmospheric pressure. Except for the MgF_2 sample which was totally inactive in this reaction, furfural conversion increased with the increase of the experiment duration (Fig. 6). The $Mg(OH)_2$ sample, which was synthesized in absence of fluorine, led to only a conversion of furfural close to 13% after 6 h of reaction. Interestingly, the presence of fluorine in solids favoured their catalytic properties for aldol condensation of furfural. Indeed, the conversions of furfural ranged between 19 and 84% after 6 hours, depending on the F/Mg ratio used, the most active being the $MgF_{1.5}(OH)_{0.5}$ sample. It can be mentioned that the difference in the specific surface area between catalysts seems not to be a key parameter to explain the difference in the catalytic properties of

the magnesium hydroxide fluorides. Indeed, $MgF_{1.5}(OH)_{0.5}$ exhibited a lower specific surface area than $MgF_{0.5}(OH)_{1.5}$, 406 and 630 $m^2\ g^{-1}$, respectively (Table 1), but the former was about 2.7 times more active than the latter (Fig. 7). In the same way, while the specific surface areas of $MgF_{1.5}(OH)_{0.5}$ and $MgF_{1.75}(OH)_{0.5}$ are very close (406 and 387 $m^2\ g^{-1}$, respectively) , the former is much more active than the latter (Fig. 7). Such a finding was already observed for several mixed-oxides using as catalysts for aldol condensation of furfural and acetone [24]. On the other hand, commercial MgO basic catalyst was also evaluated for this reaction under the same experimental conditions (without activation step). The obtained conversion was only 13% after 6h of reaction showing the interest of using hydroxide fluoride as catalyst for the aldol condensation of furfural by acetone.

The initial reaction rate of each catalyst can be evaluated by taking the tangent at the origin of each curve depicted in Fig. 6. Interestingly, a linear correlation was found between the initial reaction rate and the F/Mg molar ratio until 1.5 (Fig. 7). Indeed, an increase of the F/Mg ratio in the catalyst, between 0 and 1.5, favored the reaction rate in aldol condensation. Nevertheless, the two samples with the highest F/Mg ratios (1.75 and 2) exhibited a very limited activity. The initial reaction rate of $MgF_{1.75}(OH)_{0.25}$ was about 7 times lower than the one of $MgF_{1.5}(OH)_{0.5,}$ and MgF_2 was totally inactive. It was already reported that this type of catalyst exhibited virtually only acidity.[40,47] This is here confirmed by the characterization of acid-base properties using both CO and CO_2 probe molecules. As proposed by Kikhtyanin et al.,[26] such reaction was rather catalyzed by Brønsted acid sites explaining, at least in part, the poor catalytic properties of MgF_2 for aldol condensation of furfural. Moreover, acidic catalysts were often used in more drastic experimental conditions, between 100 °C[29,30] and 140 °C[28], i.e. at higher temperature than the one used in the present study (50 °C).

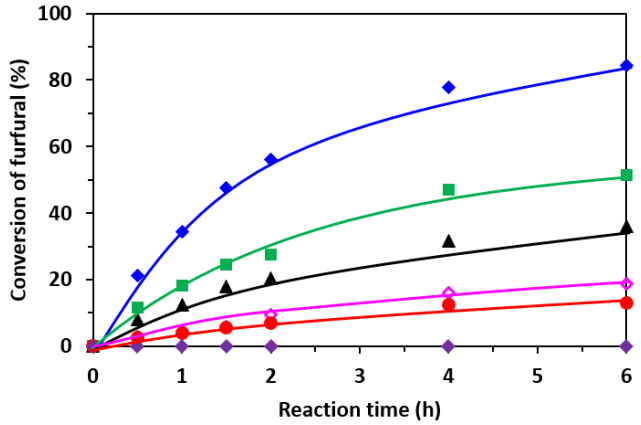

Fig. 6 Aldol condensation of furfural and acetone over magnesium hydroxide fluorides ($MgF_{2-x}(OH)_x$) at 50 °C under atmospheric pressure (furfural/acetone ratio equal to 0.5). Influence of the reaction time on the conversion of furfural. over $Mg(OH)_2$ (●), $MgF_{0.5}(OH)_{1.5}$ (▲), MgF(OH) (■), $MgF_{1.5}(OH)_{0.5}$ (◆), $MgF_{1.75}(OH)_{0.25}$ (◇) and MgF_2(◆)

A correlation was also found between the F/Mg molar ratio and the surface of the IR band at 1225 cm^{-1} measured after adsorption of CO_2 as shown in Fig. 7. As indicated in the previous part, such band corresponds to $\delta_{(OH)}$ of hydrogen carbonate species and allows to quantify the number of basic sites with moderate strength.[48–50] Consequently, the aldol condensation activity can be directly connected to the number of OH groups involved in the formation of hydrogen carbonate species deduced from CO_2 adsorption experiments. Such correlation was already reported between the activity for carbon oxysulfide hydrolysis of various mixed oxides (TiO_2-Al_2O_3, TiO_2-ZrO_2 and ZrO_2-Al_2O_3) and the intensity of the band at 1225 cm^{-1}.[48,49] As observed in Fig. 4, other basic sites are present in our samples characterized by the bands at 1358 and 1460 cm^{-1} attributed to the presence of carbonates species produced by reaction with CO_2. The intensity of these bands increases with the decrease of fluorine in the magnesium hydroxide fluoride (Fig 4), which is the opposite of the catalytic properties evolution (Fig. 7). Nevertheless, we cannot totally exclude their involvement in the aldol condensation reaction as active sites, even if their influence is probably minor.

For this reaction, the involvement of two types of active sites has been suggested: electron-donating sites (hydroxyl ions and/or oxide-ion defect) acting as reduced sites and Lewis acidic sites (coordinatively unsaturated metal site).[55] Similarly, we can propose the participation of two types of sites to explain the catalytic properties of the $MgF_{2-x}(OH)_x$ solid materials: a vacancy on magnesium present on the MgF_2 phase, acting as Lewis acid site, and hydroxyl groups with moderate strength present on $Mg(OH)_2$ phase, acting as basic site (Scheme 2). The reaction was then produced at the interface between both phases where basic and acid sites are close and it was facilitated by the probable high concentration of interfaces in these nanoscopic materials as discussed previously. Moreover, since the formation of amorphous $MgF_{2-x-y}(OH)_x(OCH_3)_y$ mixed phase cannot be excluded, some acid-pair sites can be also present on the same phase: a Lewis acid site (undercoordinated magnesium stabilized by the presence of fluorine) in the vicinity of a basic site (hydroxyl group). In order to validate this hypothesis, a mechanical mixture containing 25 wt% of $Mg(OH)_2$ and 75 wt% of MgF_2 was evaluated as catalyst for this reaction. The initial rate of this mechanical mixture was about 17 times lower than the one of the corresponding $MgF_{1.5}(OH)_{0.5}$ confirming the necessity to have neighboring sites obtained thanks to the intimate mixture of MgF_2 and $Mg(OH)_{2-x}(OCH_3)_x$ prepared by the sol-gel method used in our work.

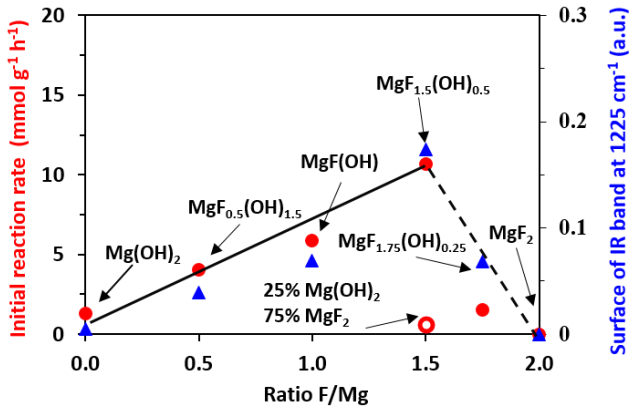

Fig. 7 Aldol condensation of furfural and acetone over magnesium hydroxide fluorides $MgF_{2-x}(OH)_x$ and over a mechanical mixture composed by 25 wt% of $Mg(OH)_2$ and 75 wt% of MgF_2 at 50 °C under atmospheric pressure (furfural/acetone ratio equal to 0.5). Effect of the F/Mg molar ratio (i) on the initial reaction rate of aldol condensation of furfural by acetone (red) and (ii) on the number of medium basic sites evaluated by the area of the band determined at 1225 cm^{-1} after CO_2 adsorption-desorption at 50 °C (blue).

The basic site can lead to the formation of carbanion species from the abstraction of the α-proton from acetone (Scheme 2). The Lewis acid site could favor the nucleophile addition onto furfural through its adsorption by the oxygen atom of the carbonyl group. Such assumption, i.e. the participation of a Lewis acid site located in the vicinity of a basic site with medium strength, to explain the catalytic properties of different mixed-oxide catalysts (Mg-Zr, Mg-Al and Ca-Zr) in aldol condensation of furfural, has been already suggested by Faba et al. [24] In addition, these authors proposed that the activity of mixed-oxide catalysts was promoted by medium-strength base sites, in accordance with our proposals.

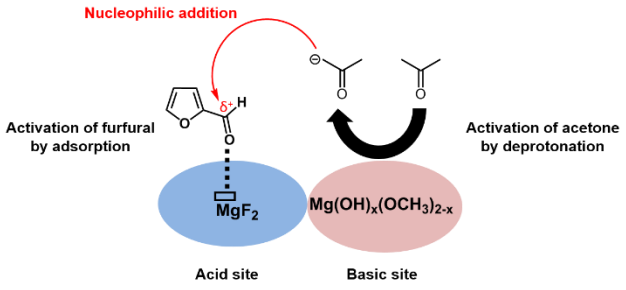

Scheme 2: Proposals concerning the active sites involved during the aldol condensation of furfural and acetone

It is very important to mention that all $MgF_{2-x}(OH)_x$ samples were used without any treatment. Indeed, as basic solids are very sensitive to ambient atmosphere by reaction with several molecules such as H_2O or CO_2, it is known that their use as basic catalysts requires a pre-treatment at a high temperature (300-800 °C depending on the solid composition and the basic site strength) before reaction in order to reveal basic sites on the catalytic surface.[56] For example, the calcination of a Mg-Al hydrotalcite material at 450 °C resulted in a doubling of the furfural conversion for its aldol condensation.[25] In addition, this activation step can lead to a drastic decrease of the specific surface area of the solid and thus of the amount of active sites. The preparation of basic solid catalysts allowing to retain basic sites without a calcination step is hence very attractive for, at least, both reasons: (i) to avoid costly heat-treatment for an industrial process, particularly for a reaction performed at low temperature (lower than 100 °C) which not requires devices adapted for high temperature, (ii) to retain high specific surface area which will be favourable to maintain high active site concentration.

Table 2: Aldol condensation of furfural and acetone at 50 °C under atmospheric pressure over magnesium hydroxide fluorides. Effect of the catalyst on the product distribution determined at the same level of conversion of furfural (close to 30%) except for $Mg(OH)_2$

Catalyst	Conv. Furfural (%)	Distribution of products (%)		
		FAc-OH	FAc	F_2Ac
$Mg(OH)_2$	13	30	35	35
$MgF_{0.5}(OH)_{1.5}$	34	16	34	50
MgF(OH)	28	19	37	44
$MgF_{1.5}(OH)_{0.5}$	34	16	36	48
$MgF_{1.75}(OH)_{0.25}$	27	17	33	50

The ability to reuse the $MgF_{1.5}(OH)_{0.5}$ sample catalyst was also investigated. For that, after 6 h of aldol condensation, the spent catalyst was filtered and dried at 90 °C during a night. The recovered catalyst was introduced in a new reaction mixture (second run). Unfortunately, the furfural conversion obtained after 6 hours during this second run was only close to 10%. This value was thus much lower than the one obtained during the first run (equal to 84%, Fig. 6) showing a strong deactivation of this kind of catalyst. As an evidence, further investigations are needed to understand the deactivation mode that occurs and to investigate experimental procedures allowing to restore their catalytic properties. Obviously, this procedure should not include heat treatment at high temperatures in order to keep the advantages of using these catalysts without activation step. This is, however, outside the topic of the present study and hence we will discuss this research topic in a forthcoming publication.

The effect of the reaction time on the conversion of furfural and on the yields of all detected products over $MgF_{1.5}(OH)_{0.5}$ is given in Fig. S2 (see ESI). As expected, three products were observed, their quantity depending on the reaction time. Accordingly with the accepted reaction route, aldol condensation of furfural and acetone over magnesium hydroxide fluorides results in the successive formation of FAc-OH (4-(furan-2-yl)-4-hydroxybutan-2-one), FAc (4-(furan-2-yl)but-3-en-2-one) and F_2Ac (1,5-di(furan-2-yl)penta-1,4-dien-3-one), as depicted in Scheme 1. Surprisingly, FAc-OH, expected as the only primary product, was detected in low quantities even at low level of furfural conversion, its yield being only equal to 4 mol% at 22 mol% of conversion (after 30 min of reaction). An increase of the reaction time led to an increase of the yield of the two other products: FAc obtained by dehydration of

FAc-OH, and F_2Ac arising from interaction of FAc-OH with another furfural molecule. Irrespective the reaction time and thus the furfural conversion, the furanic dimer (F_2Ac) was always the main product. This result can be explained by the fact that the kinetic constant of the final reaction (condensation of FAc and Furf) is much greater than the condensation of acetone and furfural yielding C8 units (initial reactions), as demonstrated by Faba et al.[24] In addition, as shown in Table 2, the selectivity of the four catalysts containing fluoride was practically independent on their fluorine content. Indeed, the main product was always the furanic dimer, its amount being close to 50 mol% irrespective of the catalyst. As F_2Ac is a more bulky molecule compared to FAc, the fact that the former was favoured compared to the latter over magnesium hydroxide fluoride catalysts seems to indicate the absence of diffusion limitations over these mesoporous catalysts. It is important to emphasize that diacetone alcohol produced by aldol condensation of acetone was never detected in our experimental conditions.

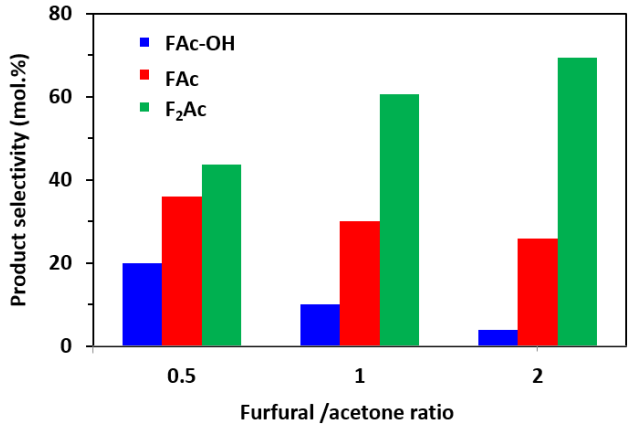

Fig. 8 Aldol condensation of furfural and acetone over $MgF_{1.5}(OH)_{0.5}$ at 50 °C under atmospheric pressure. Influence of the furfural/acetone ratio on the distribution of products at iso-conversion of furfural (close to 20%)

The influence of the composition of reactants feed on the catalytic properties of $MgF_{1.5}OH_{0.5}$ was also investigated. It can be observed that the molar ratio of reactants for aldol condensation plays a significant role in both the activity and the selectivity of the catalyst. Indeed, Fig. S3 (see ESI) shows that the presence of an excess of acetone favours the consumption of furfural by aldol condensation. Actually, with the same initial molar quantity of furfural (5 mmol), the use of a furfural/acetone ratio equal to 0.5 allowed to convert more than 4 mmol of furfural after 6 hours while the use of a furfural/acetone molar ratio equal to 2 led only to the transformation of 1.3 mmol of furfural. As an evidence, the conversion of furfural is limited to 50% in the latter case. Consequently a higher furfural/acetone ratio diminishes considerably the initial reaction rate (from 10.7 to 2.5 mmol g^{-1} h^{-1}) since an excess of furfural may engender unnecessary adsorption on Lewis acid sites and thereby could inhibit the access of acetone to the neighbour basic sites. As a result, less active carbanions species can be formed when an excess of furfural was used and hence restraining its transformation. However, an excess of furfural led to a better selectivity on furanic dimer (F_2Ac) as highlighted in Fig. 8. Indeed, when the molar ratio of furfural/acetone was increased from 0.5 to 2, the selectivity for the formation of dimer species (F_2Ac) increased by 38%.

Conclusions

It was demonstrated that magnesium hydroxide fluorides $MgF_{2-x}(OH)_x$ can be used as efficient catalysts without preliminary thermal activation for aldol condensation of furfural and acetone under mild conditions (50 °C, under atmospheric pressure). A strong effect of the F/Mg molar ratio used during the synthesis of fluorides on their catalytic properties was highlighted. An optimum was determined for a F/Mg ratio equal to 1.5. This optimum was attributed to the presence of an intimate mixture of MgF_2 and $Mg(OH)_2$ phases allowing to create active sites combined an under-coordinated magnesium in the MgF_2 phase, acting as Lewis acid site, in the vicinity of hydroxyl groups with moderate strength in $Mg(OH)_{2-x}(OCH_3)_x$ phase. Moreover, it was highlighted that the presence of fluorine allows to stabilize the basic sites with moderate strength at ambient temperature, allowing to use these catalysts without pre-treatment of activation, a great benefit for an industrial point of view. Such hydroxide fluoride catalyst favored the C13 dimer species, particularly in excess of furfural. The present work confirms the potential of nanosized magnesium hydroxide fluorides as heterogeneous acid-base catalysts for aldol condensation reactions. The easy tuning of their acid-base properties and their high specific surface area make them attractive for other reactions involved in catalytic processes.

Conflicts of interest

There are no conflicts to declare.

Acknowledgements

Minrui Xu acknowledges a PhD fellowship from Solvay. Stéphane Célerier, Frédéric Richard and Jean-Marc Clacens acknowledge financial support from the European Union (ERDF) and “Region Nouvelle Aquitaine”.

Notes and references

1 A. Corma, S. Iborra and A. Velty, *Chem. Rev.*, 2007, **107**, 2411–2502.
2 G. W. Huber, S. Iborra and A. Corma, *Chem. Rev.*, 2006, **106**, 4044–4098.
3 H. Kobayashi and A. Fukuoka, *Green Chem.*, 2013, **15**, 1740–1763.
4 S. Dutta, S. De, B. Saha and M. I. Alam, *Catal. Sci. Technol.*, 2012, **2**, 2025–2036.
5 M. J. Climent, A. Corma and S. Iborra, *Green Chem.*, 2014, **16**, 516–547.
6 I. Delidovich, K. Leonhard and R. Palkovits, *Energy Environ. Sci.*, 2014, **7**, 2803–2830.
7 W. Xu, H. Wang, X. Liu, J. Ren, Y. Wang and G. Lu, *Chem. Commun.*, 2011, **47**, 3924–3926.

8 L. Bui, H. Luo, W. R. Gunther and Y. Román-Leshkov, *Angew. Chem. Int. Ed.*, 2013, **52**, 8022–8025.
9 J. Wu, G. Gao, J. Li, P. Sun, X. Long and F. Li, *Applied Catalysis B: Environmental*, 2017, **203**, 227–236.
10 Z. J. Brentzel, K. J. Barnett, K. Huang, C. T. Maravelias, J. A. Dumesic and G. W. Huber, *ChemSusChem*, 2017, **10**, 1351–1355.
11 H. Li, A. Riisager, S. Saravanamurugan, A. Pandey, R. S. Sangwan, S. Yang and R. Luque, *ACS Catal.*, 2018, **8**, 148–187.
12 R. M. West, Z. Y. Liu, M. Peter and J. A. Dumesic, *ChemSusChem*, 2008, **1**, 417–424.
13 R. Xing, A. V. Subrahmanyam, H. Olcay, W. Qi, G. P. van Walsum, H. Pendse and G. W. Huber, *Green Chem.*, 2010, **12**, 1933–1946.
14 J. Yang, N. Li, S. Li, W. Wang, L. Li, A. Wang, X. Wang, Y. Cong and T. Zhang, *Green Chem.*, 2014, **16**, 4879–4884.
15 Q. Xia, Y. Xia, J. Xi, X. Liu and Y. Wang, *Green Chem.*, 2015, **17**, 4411–4417.
16 R. Ramos, Z. Tišler, O. Kikhtyanin and D. Kubička, *Catal. Sci. Technol.*, 2016, **6**, 1829–1841.
17 L. Faba, E. Díaz and S. Ordóñez, *Applied Catalysis B: Environmental*, 2014, **160–161**, 436–444.
18 L. Faba, E. Díaz and S. Ordóñez, *Catal. Sci. Technol.*, 2015, **5**, 1473–1484.
19 L. Faba, E. Díaz, A. Vega and S. Ordóñez, *Catalysis Today*, 2016, **269**, 132–139.
20 R. Ramos, Z. Tišler, O. Kikhtyanin and D. Kubička, *Applied Catalysis A: General*, 2017, **530**, 174–183.
21 N. Fakhfakh, P. Cognet, M. Cabassud, Y. Lucchese and M. D. de Los Ríos, *Chemical Engineering and Processing: Process Intensification*, 2008, **47**, 349–362.
22 W. Shen, G. A. Tompsett, K. D. Hammond, R. Xing, F. Dogan, C. P. Grey, W. C. Conner, S. M. Auerbach and G. W. Huber, *Applied Catalysis A: General*, 2011, **392**, 57–68.
23 I. Sádaba, M. Ojeda, R. Mariscal, J. L. G. Fierro and M. L. Granados, *Applied Catalysis B: Environmental*, 2011, **101**, 638–648.
24 L. Faba, E. Díaz and S. Ordóñez, *Applied Catalysis B: Environmental*, 2012, **113**, 201–211.
25 D. Nguyen Thanh, O. Kikhtyanin, R. Ramos, M. Kothari, P. Ulbrich, T. Munshi and D. Kubička, *Catalysis Today*, 2016, **277**, 97–107.
26 O. Kikhtyanin, V. Kelbichová, D. Vitvarová, M. Kubů and D. Kubička, *Catalysis Today*, 2014, **227**, 154–162.
27 M. Su, W. Li, T. Zhang, H. Xin, S. Li, W. Fan and L. Ma, *Catal. Sci. Technol.*, 2017, **7**, 3555–3561.
28 H. Li, Z. Xu, P. Yan and Z. C. Zhang, *Green Chem.*, 2017, **19**, 1751–1756.
29 O. Kikhtyanin, D. Kubička and J. Čejka, *Catalysis Today*, 2015, **243**, 158–162.
30 S. Rojas-Buzo, P. García-García and A. Corma, *Green Chem.*, 2018, **20**, 3081–3091.
31 S. Célérier and F. Richard, *Catalysis Communications*, 2015, **67**, 26–30.
32 E. Kemnitz, *Catal. Sci. Technol.*, 2015, **5**, 786–806.
33 F. Frouri, S. Célérier, P. Ayrault and F. Richard, *Applied Catalysis B: Environmental*, 2015, **168**, 515–523.
34 S. M. Coman, S. Wuttke, A. Vimont, M. Daturi and E. Kemnitz, *Advanced Synthesis & Catalysis*, 2008, **350**, 2517–2524.
35 H. A. Prescott, Z.-J. Li, E. Kemnitz, J. Deutsch and H. Lieske, *J. Mater. Chem.*, 2005, **15**, 4616–4628.
36 M. Wojciechowska, A. Wajnert, I. Tomska-Foralewska, M. Zieliński and B. Czajka, *Catal Lett*, 2009, **128**, 77–82.
37 I. Tomska-Foralewska, M. Zieliński, M. Pietrowski, W. Przystajko and M. Wojciechowska, *Catalysis Today*, 2011, **176**, 263–266.
38 M. Zieliński, I. Tomska-Foralewska, M. Pietrowski, W. Przystajko and M. Wojciechowska, *Catalysis Today*, 2012, **191**, 75–78.
39 M. Zieliński, A. Kiderys, M. Pietrowski, I. Tomska-Foralewska and M. Wojciechowska, *Catalysis Communications*, 2016, **76**, 54–57.
40 S. Célerier, S. Morisset, I. Batonneau-Gener, T. Belin, K. Younes and C. Batiot-Dupeyrat, *Applied Catalysis A: General*, 2018, **557**, 135–144.
41 G. Scholz, C. Stosiek, M. Feist and E. Kemnitz, *Eur. J. Inorg. Chem.*, 2012, **2012**, 2337–2340.
42 R. E. O'Neill, L. Vanoye, C. De Bellefon and F. Aiouache, *Applied Catalysis B: Environmental*, 2014, **144**, 46–56.
43 A. A. Rywak, J. M. Burlitch and T. M. Loehr, *Chem. Mater.*, 1995, **7**, 2028–2038.
44 Y. Diao, W. P. Walawender, C. M. Sorensen, K. J. Klabunde and T. Ricker, *Chem. Mater.*, 2002, **14**, 362–368.
45 S. Wuttke, A. Vimont, J.-C. Lavalley, M. Daturi and E. Kemnitz, *J. Phys. Chem. C*, 2010, **114**, 5113–5120.
46 I. Agirrezabal-Telleria, Y. Guo, F. Hemmann, P. L. Arias and E. Kemnitz, *Catal. Sci. Technol.*, 2014, **4**, 1357–1368.
47 F. Richard, S. Célérier, M. Vilette, J.-D. Comparot and V. Montouillout, *Applied Catalysis B: Environmental*, 2014, **152–153**, 241–249.
48 C. Lahousse, A. Aboulayt, F. Maugé, J. Bachelier and J. C. Lavalley, *Journal of Molecular Catalysis*, 1993, **84**, 283–297.
49 C. Lahousse, F. Maugé, J. Bachelier and J.-C. Lavalley, *J. Chem. Soc., Faraday Trans.*, 1995, **91**, 2907–2912.
50 J. Szanyi and J. H. Kwak, *Phys. Chem. Chem. Phys.*, 2014, **16**, 15117–15125.
51 K. I. Hadjiivanov and G. N. Vayssilov, in *Advances in Catalysis*, Academic Press, 2002, vol. 47, pp. 307–511.
52 T. Krahl, A. Vimont, G. Eltanany, M. Daturi and E. Kemnitz, *J. Phys. Chem. C*, 2007, **111**, 18317–18325.
53 A. Astruc, C. Cochon, S. Dessources, S. Célérier and S. Brunet, *Applied Catalysis A: General*, 2013, **453**, 20–27.
54 S. Wuttke, S. M. Coman, J. Kröhnert, F. C. Jentoft and E. Kemnitz, *Catalysis Today*, 2010, **152**, 2–10.
55 M. Akimoto and I. G. D. Lana, *Journal of Catalysis*, 1980, **62**, 84–93.
56 H. Hattori, *Applied Catalysis A: General*, 2015, **504**, 103–109.

